ANTIMICROBIAL AGENTS AND CHEMOTHERAPY, Dec. 2011, p. 5753–5760 Vol. 55, No. 12
0066-4804/11/$12.00 doi:10.1128/AAC.00724-11

Zinc Pyrithione Inhibits Yeast Growth through Copper Influx and Inactivation of Iron-Sulfur Proteins▽†

Nancy L. Reeder,[1] Jerry Kaplan,[2] Jun Xu,[1] R. Scott Youngquist,[1] Jared Wallace,[2] Ping Hu,[1] Kenton D. Juhlin,[1] James R. Schwartz,[3] Raymond A. Grant,[1] Angela Fieno,[1] Suzanne Nemeth,[1] Tim Reichling,[1] Jay P. Tiesman,[1] Tim Mills,[4] Mark Steinke,[3] Shuo L. Wang,[1] and Charles W. Saunders[1]*

Procter & Gamble Co., Miami Valley Innovation Center, Cincinnati, Ohio[1]; Department of Pathology, 50 N. Medical Drive, School of Medicine, University of Utah, Salt Lake City, Utah[2]; Procter & Gamble Co., Sharon Woods Innovation Center, Cincinnati, Ohio[3]; and Procter & Gamble Co., Fabric & Home Care Innovation Center, Cincinnati, Ohio[4]

Received 25 May 2011/Returned for modification 23 July 2011/Accepted 14 September 2011

Zinc pyrithione (ZPT) is an antimicrobial material with widespread use in antidandruff shampoos and antifouling paints. Despite decades of commercial use, there is little understanding of its antimicrobial mechanism of action. We used a combination of genome-wide approaches (yeast deletion mutants and microarrays) and traditional methods (gene constructs and atomic emission) to characterize the activity of ZPT against a model yeast, *Saccharomyces cerevisiae*. ZPT acts through an increase in cellular copper levels that leads to loss of activity of iron-sulfur cluster-containing proteins. ZPT was also found to mediate growth inhibition through an increase in copper in the scalp fungus *Malassezia globosa*. A model is presented in which pyrithione acts as a copper ionophore, enabling copper to enter cells and distribute across intracellular membranes. This is the first report of a metal-ligand complex that inhibits fungal growth by increasing the cellular level of a different metal.

Fungi have an essential role in causing dandruff, a scalp disease affecting >40% of the world's adult population (36). Zinc pyrithione (ZPT) is an antimicrobial compound that has been used since the 1960s in antidandruff shampoos (36) and in antifouling paints (37). In dandruff subjects, ZPT treatment reduces the amount of fungus on the scalp and stops dandruff flaking (6). Despite billions of human scalp treatments for over 4 decades, little is known of the mechanism by which ZPT inhibits fungal growth.

Malassezia globosa and *M. restricta* are the two most common fungi on scalp (15). Despite a recent description of the genome sequences of these two species (42), study of *Malassezia* is challenging due to the absence of transformation methods and available mutants. Several attempts have been made to characterize the mode of action of ZPT against model fungi. ZPT has been reported to inhibit transport by membrane depolarization (5, 11). However, efficacy was reported only with doses of at least 100 μM, whereas microbial growth inhibition is observed at much lower ZPT doses. Pyrithione is a well-known zinc ionophore that causes increased zinc levels within mammalian cells (1, 18, 27). High intracellular zinc levels can inhibit microbial growth, likely due to zinc binding to intracellular proteins and resulting in mismetallation (31). Yasokawa et al. (43) recently used transcriptional analysis of ZPT-treated *Saccharomyces cerevisiae* to suggest that ZPT causes iron starvation. They further showed that an iron salt lowered the anti-yeast activity of ZPT, suggesting that iron starvation is a key component of ZPT's mechanism of action.

In this communication, we confirm the observation by Yasokawa et al. (43) that ZPT increases transcription of the iron regulon: however, we ascribe that increase not to a transcriptional response to low iron concentrations but rather to a decrease in the activity of iron-sulfur (Fe-S) cluster-containing proteins. We show that ZPT-mediated growth inhibition is due to increased copper uptake and that copper inactivates key Fe-S proteins by a mechanism similar to that described for copper-mediated growth inhibition in bacteria (7, 26). Further, we show that ZPT incubation with the scalp fungus *M. globosa* also leads to a copper imbalance, suggesting that increased intracellular copper is the source of ZPT efficacy against the fungi associated with dandruff.

MATERIALS AND METHODS

Strains. *M. globosa* 7966 was obtained from the Centraalbureau voor Schimmelcultures, Utrecht, The Netherlands. *S. cerevisiae* cultures were grown in the rich medium yeast extract-peptone-dextrose (YPD) or synthetic yeast nitrogen base (YNB) media and synthetic complete media (CM) (Becton Dickinson, Sparks, MD). The *S. cerevisiae* strains used in the study are listed in Table 1.

The hypomorphic strains were derivatives of DY150 or DY1457 as indicated in the figure legends in the supplemental materials. These strains carry recessive mutations complemented by the indicated gene on a low-copy-number plasmid (19). The genetic defect of the *NFS1* hypomorphic strain was found to encode a change in a conserved proline of Nfs1, at residue 478, to leucine.

Chemicals. Arch Chemicals (Norwalk, CT) supplied CuPT and ZPT (two-μm particles, as used in Head & Shoulders shampoo). Octopirox, also called piroctone [1-hydroxy-4-methyl-6-(2,4,4-trimethylpentyl)-2(1H)-pyridone] olamine, was from Clariant (Charlotte, NC). These materials were prepared in dimethyl sulfoxide (DMSO). Other chemicals were from Sigma Chemical Company (St. Louis, MO) unless otherwise noted.

Enzyme assays. For aconitase assays of BY4741 lysates, an overnight culture was diluted to an optical density (OD) at 600 nm of 0.1. After it reached an OD of 0.2, the culture was treated with ZPT and incubated overnight at 30°C. The cells were collected by centrifugation and washed and concentrated 20-fold by

* Corresponding author. Mailing address: Miami Valley Innovation Center, Procter & Gamble Co., P.O. Box 538707, Cincinnati, OH 45253-8707. Phone: (513) 627-2089. Fax: (513) 627-1259. E-mail: saunders.cw@pg.com.

† Supplemental material for this article may be found at http://aac.asm.org/.

▽ Published ahead of print on 26 September 2011.

TABLE 1. *S. cerevisiae* strains used in the study

Strain	Genotype	Source or reference
BY4741	*his3Δ1 leu2Δ met15Δ0 ura3Δ0 MAT***a**	Open Biosystems
BY4742	*his3Δ1 leu2Δ0 lys2Δ0 ura3Δ0 MAT*α	Open Biosystems
W303	*leu2-3,112 trp1-1 can1-100 ura3-1 ade2-1 his3-11,15* [*phi*$^+$] *MAT***a**/*MAT*α	
DY150	*ura3-52 leu2-3 trp2-1 his3-11 can1-100* (*oc*) *ade2 mat***a**	Felice et al., 2005 (12)
DY1457	*ura3-52 leu2-3 trp2-1 his3-11 can1-100* (*oc*) *ade2 mat*α	Felice et al., 2005 (12)
DY150 (FET3-GFP)	*ura3-52 leu2-3 trp2-1 his3-11 can1-100* (*oc*) *ade2 mat***a** *FET3-GFP*::*KanMX*	Felice et al., 2005 (12)
Δzrc1Δcot1 DY150	*ura3-52, leu2-3, 112, trp1-1, his3-11, ade2-1, can1-100*(*oc*), Δ*zrc1*::*HIS3*, Δ*cot1*::*KanMX*	Lin et al., 2008 (22)
OCY356	Derived from W303: *ura3-52, leu2-3, trp2-1, his3-11, can1-100*(*oc*), *ade6, ho*::*FET3-lacZ, mat***a**	Kumánovics et al., 2008 (19)
OCY357	Derived from W303: *ura3-52, leu2-3, trp2-1, his3-11, can1-100*(*oc*), *ade6, ho*::*FET3-lacZ, mat*α	Kumánovics et al., 2008 (19)

suspension in 100 mM NaCl–20 mM Tris (pH 7.4). The cells were lysed using glass beads for 10 cycles of vortexing (1 min) and chilling on ice (1 min). After centrifugation, the supernatant was recovered. Cell lysate (50 μl) was assayed in a 200-μl volume in a 96-well plate (UV-transparent Corning 3679 plate) using a Bioxytech Aconitase-340 kit (OxisResearch) according to instructions. Samples were incubated for 5 min at 37°C, with the results based on the increase in OD (at 340 nm) in the interval from 1 to 5 min. For each sample, a background was subtracted based on the measurements determined when $NADP^+$ was not added. Total protein was measured using a Micro BCA kit (Thermo Scientific, Rockford, IL). Aconitase specific activity was measured as micromoles of product formed per minute per milligram of protein.

All other enzyme assays were performed using lysates of DY150 (or its derivative) grown in Sabouraud's dextrose (SD) media at 30° for 5 h with various concentrations of ZPT. Levels of isopropylmalate isomerase (Leu1) were assayed using DY150 harboring a *LEU2*-containing plasmid to restore the leucine biosynthesis pathway and increase Leu1 activity. Cells were harvested at OD values between 0.5 and 1.0 and then lysed.

Specific activity units are reported as the change in the NADH level in micromoles per minute per milligram of protein. Alcohol dehydrogenase (ADH) was extracted and assayed as described previously (4). Aconitase was extracted and assayed as described previously (20), using 8 U (the optical density of a 1-ml sample multiplied by the culture volume in milliliters) of cells and 8 μl of extract for the assay, with aconitase-specific activity calculated as published previously (20).

To prepare lysates for the malate dehydrogenase assays, an extract was prepared by washing 8 U of cells once in water and once in 0.1 M potassium phosphate (pH 7.4)–1 mM phenylmethylsulfonyl fluoride. The pellet was then suspended in 300 μl of the buffer, and an equal volume of acid-washed glass beads was added. The Eppendorf tubes were then subjected to vortexing for 1 min at 4°C five times, with a 1-min cooling interval after each vortex procedure. The tubes were spun at 3,000 × *g* for five min, and the supernatant was saved as the cell extract. The malate dehydrogenase activity assay was performed as described previously (34).

To prepare lysates for the glutamate synthase assays, extracts were prepared as described above for the malate dehydrogenase assays except that 10 to 20 U of cells were used and the buffer pH was 7.5. Glutamate synthase was assayed as described previously (35).

For Leu1, the cells were extracted and the assay was performed as described previously (30). The Leu1 activity was determined by the increase of absorbance at 235 nm (representing a double bond of the intermediate). We used the same equation for calculating specific activity but substituted the molar extinction coefficient for a double bond (4.530 $mmol^{-1}$ l for a 1.0-cm path length) for the molar extinction coefficient of NADH.

Atomic emission. A BY4741 overnight culture was used to inoculate YPD at an OD of 0.1, and the culture was incubated at 30°C. Once the OD reached 0.2, the culture was treated with test materials and incubated 20 h for aerobic cultures or 3 days for anaerobic cultures. Cells were harvested by centrifugation, and the pellets were washed twice with 50 mM Tris (pH 6.5)–10 mM EDTA. After the wash fluid was removed, the pellets were lyophilized. One liter of cells, at an OD of 1 (measured in a 1-cm cuvette), corresponded to 7 g of dried cell mass. Where indicated, W303 cultures were incubated for 10 h in YPD medium and the samples were prepared as described above.

M. globosa was inoculated at an OD of 0.1 into minimal medium (15 mM NH_4Cl, 6.6 mM KH_2PO_4, 0.5 mM K_2HPO_4, 1.7 mM sodium chloride, 0.7 mM $CaCl_2$, 2 mM $MgCl_2$, 0.5 μg/ml boric acid, 0.04 μg/ml $CuCl_2$, 0.1 μg/ml KI, 0.19 μg/ml $ZnCl_2$, 0.05 μg/ml $FeCl_2$, 400 μg/ml $MnCl_2$, 2% glucose, 0.5 mM cysteine, 1% Tween 40, 0.1% yeast extract, 2 μg/ml calcium pantothenate, 2 μg/ml thiamine, 0.02 μg/ml biotin, 20 μg/ml inositol, 2 μg/ml pyridoxine, 2 μg/ml folic acid, 400 μg/ml niacin, 200 μg/ml *p*-aminobutyric acid, 200 μg/ml riboflavin, 200 μg/ml sodium molybdate) and treated with test materials. The cultures were incubated at 30°C with shaking for 4 days. The cells were harvested by centrifugation and washed four times with 10 ml of 0.9% sodium chloride–0.4% Dawn (Procter & Gamble) to remove residual lipid from the culture medium and then washed twice with 10 ml of 0.9% sodium chloride. The fluid was removed, and the cells were lyophilized.

The lyophilized cell pellets were suspended in concentrated nitric acid and transferred to Teflon digestion vessels. The process was repeated twice with a total of 10 ml of nitric acid. A 50-μl volume of yttrium (1 mg/ml) was added as an internal standard. The vessels were sealed and microwave digested using a Milestone (Shelton, CT) Ethos EZ station and the following conditions: 3 min for a temperature increase to 90°C, 2 min at 90°C, a temperature increase over 3 min to 145°C, 4 min at 145°C, a temperature increase over 3 min to 190°C, and 15 min at 190°C. The samples were diluted to 50 ml with deionized water and analyzed for Cu, Fe, S, and Zn content by the use of inductively coupled plasma optical emission spectrometry (Optima 5300 DV instrument; PerkinElmer, Waltham, MA). Concentrations were measured against standards ranging from 10 ppb to 20 ppm. Concentrations were calculated in parts per million relative to the dried sample weights and dilution volume (50 ml).

Testing growth inhibition. In experiments performed with *S. cerevisiae*, 50% inhibitory concentrations (IC_{50}s) were obtained by adding 5 μl of an overnight culture to a well with up to 5 μl of a test material in 190 μl of YPD medium in a 96-well plate (Costar 3596). Cultures were incubated without shaking overnight at 30°C. To prevent evaporation, the plates were humidified by placing wet cotton batting around the plates. At the end of the growth period, samples were shaken for 30 s on an Eppendorf MixMate plate shaker, and the optical density (OD) at 600 nm was measured using a SpectraMax Plus plate reader (Molecular Devices, Sunnyvale, CA). In the OD ranges of these experiments, an OD measured in the 96-well plate reader corresponded to about 60% of the value that would have been measured for the same sample in a cuvette in a Beckman DU 640 spectrophotometer.

For the deletion library, stock plates were completely thawed and thoroughly mixed. Cultures (5 μl) were transferred to wells with YPD medium (200 μl) and incubated for 2 days as described above. The culture (5 μl) was used to inoculate YPD medium (190 μl) containing the test compound (5 μl). Plates were incubated overnight as described above, and the OD was measured as described above.

Each of the deletion mutants was tested individually using three concentrations of ZPT (2.5, 5, and 10 μM), two doses of zinc chloride (1.1 and 2.2 mM), and a DMSO control at 2.5%.

An initial partial ranking of the deletion mutants was based on a Jonckheere-Terpstra test (17) to determine a trend of decreased growth at increasing ZPT concentrations, using the values for responses to each of the three ZPT concentrations and the DMSO control. Since only four samples were used in this test, there were only a few possibilities (0.0208, 0.0355, 0.0871, 0.1393, 0.2484, 0.3590, and 1) for the one-sided *P* values.

The 180 deletion mutants whose growth was reduced 50% by ZPT treatment were ranked within each of the *P* value bins by a simple estimate of their ED_{50} (the dose at which a 50% reduction in growth was achieved). This estimate was a linear interpolation between the doses that bracketed the 50% reduction. The same approach was used to rank the 328 strains whose growth was reduced 50% by each of the doses of zinc chloride. The deletion mutants were ranked according to their ED_{50} values.

The sensitivity to ZPT of the W303-based strains was determined by growth overnight in liquid medium or by dilution plating.

M. globosa does not grow well in 96-well plates, so growth inhibition was tested using 50-ml tubes with 10 ml of mDixon medium (9). Cultures were inoculated

to an OD of 0.2 and challenged with test material. After 48 h of shaking at 30°C, the OD was measured.

Gene constructs and miscellaneous methods. *CTR1-LacZ* and *CUP1-LacZ* constructs were obtained from Dennis Winge (University of Utah). *ZRE-lacZ* was generated as described previously (45) and was the generous gift of David Eide. Strains with *FET3-GFP* integrated were as described previously (12). Iron uptake assays were performed as described previously (8). Additional information can be found in Materials and Methods in the supplemental material.

RESULTS

ZPT induces the *S. cerevisiae* iron regulon but not through copper depletion or decreased iron transport. Yasokawa et al. (43) showed that ZPT induced expression of the iron regulon, the set of transcripts regulated by the low-iron concentration-sensing transcription factor Aft1. We also observed this result in microarray experiments (see Table S1 in the supplemental material) and confirmed the microarray data by showing induction of a *FET3-lacZ* reporter (Fig. 1a). One explanation for the increased expression of the iron regulon is that ZPT lowers the activity of the high-affinity iron transport system by chelation of copper from the Fet3 ferroxidase that forms a complex with the transmembrane permease Ftr1. A decrease in Fet3/Ftr1-mediated iron acquisition would result in decreased cytosolic iron levels and induction of the iron regulon (2). However, ZPT treatment induced the expression of a Fet3-GFP chimera which was localized to the cell surface even in iron-replete medium, further confirming ZPT induction of the iron regulon (Fig. 1b). Furthermore, high-affinity iron uptake was increased in ZPT-treated cells (Fig. 1c). The rate of iron uptake was little affected by the presence of added copper, indicating that the cell surface Fet3 was fully loaded with copper (8, 13). In summary, the iron regulon induction by ZPT was not due to impaired iron uptake.

Another explanation for the ZPT-mediated induction of the iron regulon is that ZPT removes copper from the Sod1 cytosolic superoxide dismutase, whose inactivation is known to induce expression of the iron regulon and decrease viability under aerobic conditions (10). However, there was no discernible effect of ZPT on Sod1 activity until application of a ZPT dose (15 μM) that was higher than the dose that provided 50% growth inhibition (5 μM) (see Fig. S1A in the supplemental material). Furthermore, ZPT was similarly potent under anaerobic conditions in which superoxide dismutase is not required (Fig. 2a). Therefore, the ZPT-mediated induction of the iron regulon was not due to loss of Sod1 activity. In addition, the finding that ZPT is as effective anaerobically as aerobically suggests that the mechanism of ZPT toxicity is not due to increased oxidative damage.

We used atomic emission spectroscopy of ZPT-treated cells to test for iron starvation and search for other metal imbalances. Iron levels showed little or no change upon ZPT treatment (Fig. 2b). In contrast, other treatments using, e.g., EDTA and bathophenanthroline disulfonate (BPS) provoked considerable iron starvation and induced little or no growth inhibition (see Table S2 in the supplemental material); thus, iron starvation does not explain ZPT's mechanism of action.

Gene expression data indicate ZPT-mediated changes in cytosolic copper. Atomic absorption analysis showed that ZPT treatment resulted in a significant increase in cellular copper levels and, at most, only a small increase in zinc. The microarray data from both Yasokawa et al. (43) and our studies (see Table S1 in the supplemental material) show that the *CTR1* copper importer gene is among the five genes most downregulated by ZPT treatment, suggesting that cellular copper levels were increased by ZPT treatment. The *CUP1* copper metallothionein gene showed a slight increase in expression, although not as much as when cells are exposed to copper salts (16, 39,

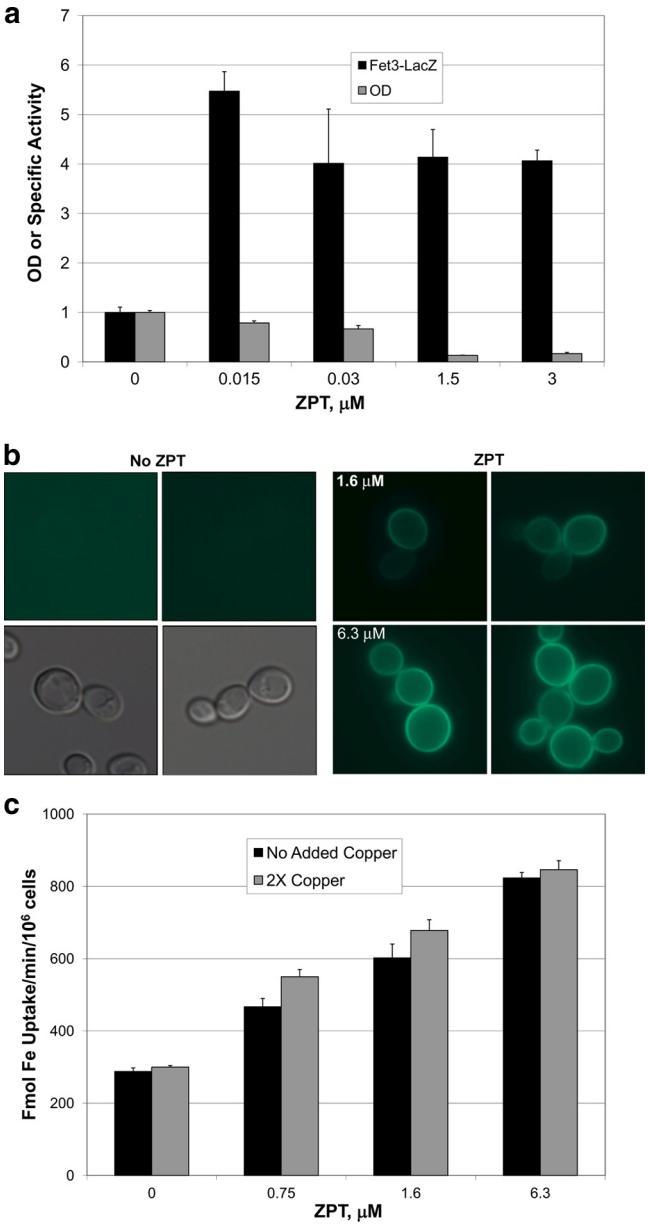

FIG. 1. Iron transport activity is not impaired by ZPT. (a) Fet3-LacZ activity and growth inhibition of DY1457 cells grown in CM with the indicated dose of ZPT. (b) Fluorescence from a Fet3-GFP chimeric protein with DY150 (*FET3-GFP*) yeast grown in YPD medium in the absence or presence of ZPT. The images at the lower left were produced using visible light; the other images were produced using fluorescent light. (c) DY150 (*FET3-GFP*) was incubated in YPD medium with 0.15 μM iron and 1 mM ascorbate in the presence or absence of added copper (0.25 μM CuSO4; described as 2× copper in the legend). Cultures were inoculated at an OD of 0.3 and grown for 6 h, whereupon ^{59}Fe was added to the medium and radioactive iron uptake was measured.

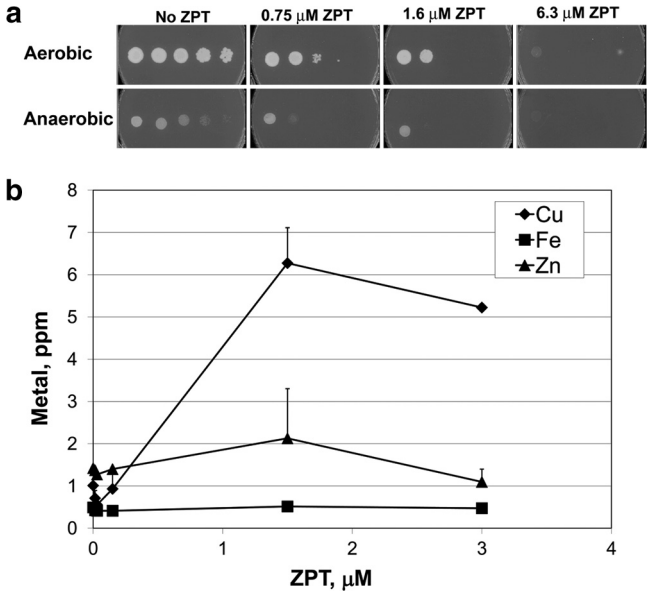

FIG. 2. ZPT is similarly potent under anaerobic and aerobic conditions and causes a metal imbalance. (a) DY1457 was grown in YPD medium and spotted onto YPD plates with the indicated amount of ZPT. Cultures were incubated for 69.5 h under either aerobic or anaerobic conditions. (b) Atomic emission of *S. cerevisiae* W303 in response to ZPT. Cultures were grown aerobically for 10 h in YPD medium.

44). Exposure of cells to ZPT resulted in decreased *CTR1-lacZ* expression (see Fig. S1B in the supplemental material) and slightly increased *CUP1-lacZ* expression (see Fig. S1C in the supplemental material). Taken together, these data suggest an increase in cytosolic copper levels.

The results of yeast deletions indicated that ZPT inhibits growth through increased levels of copper but not zinc. From these data, it seems possible that ZPT's primary effects on cells are due to an imbalance of copper, zinc, and iron. To distinguish among the effects of these metals, we performed a genome-wide survey of ZPT-mediated growth inhibition in the ~4,700-member haploid deletion collection. ZPT-sensitive strains should carry deletions within genes whose products (i) protect the cells from ZPT or (ii) comprise part of a pathway that is a primary target for ZPT. As a control, we used zinc chloride to test the deletion library members and found that the 12 most zinc chloride-sensitive mutants were defective in the vacuolar ATPase (see Table S3 in the supplemental material) required for zinc resistance resulting from sequestration of zinc into the vacuole (28, 33). Each of these 12 mutants was also found to be sensitive to zinc chloride in the deletion library screening (28). These results indicate that our library screening for zinc chloride sensitivity produced results consistent with the published literature.

If ZPT inhibits yeast growth through increased intracellular zinc levels, we would expect similar patterns of growth defects in the deletion strain experiments performed with ZPT and zinc chloride. However, this was not the case (see Table S3 in the supplemental material): 11 of the 12 most zinc chloride-sensitive vacuolar ATPase mutants were not among the 180 most ZPT-sensitive strains. As an additional test of the possible role of zinc in ZPT-mediated growth inhibition, we tested a mutant deleted for both *ZRC1* and *COT1*, as such a mutant is missing both known vacuolar zinc transporters and is highly sensitive to zinc salts (24). The double mutant was no more sensitive to ZPT than the wild-type cell (see Fig. S2A in the supplemental material). Therefore, ZPT-mediated growth inhibition is not due to increased intracellular zinc levels.

The ninth most ZPT-sensitive strain carries a deletion for *ACE1*, a transcription factor that protects cells from high levels of copper (29). The observed ZPT sensitivity of the *ACE1* deletion mutant was not an accidental artifact: the mutant deleted for YGL165C, annotated as "dubious open reading frame, partially overlaps *CUP2*," a synonym for *ACE1* (*Saccharomyces* genome database; http://www.yeastgenome.org), was ranked sixth. The presence of two *ACE1*-deleted strains among the most ZPT-sensitive strains suggests that *ACE1* protects cells from ZPT. In contrast, neither of these mutants was in the top 40% among zinc chloride-sensitive strains. We further evaluated the *ACE1* deletion and wild-type control strain and found that the *ACE1* deletion mutant was 11-fold more sensitive to ZPT (Fig. 3a) and 10-fold more sensitive to copper chloride but not more sensitive to zinc chloride (see Table S4 in the supplemental material). Introduction of an *ACE1*-containing plasmid into an *ACE1* deletion mutant restored wild-type sensitivity to ZPT (see Fig. S2B in the supplemental material). The *ACE1* deletion conferred sensitivity to other pyrithione salts beyond ZPT. Copper pyrithione (CuPT) and sodium pyrithione were each more potent against an *ACE1*-deleted strain (see Table S4 in the supplemental material). In contrast, other metal-binding antiyeast agents (1,10-phenanthroline, octopirox, EDTA, and bathophenanthroline disulfonate [BPS]) were similarly potent against the wild-type and *ACE1*-deleted strains (see Table S4 in the supplemental material), demonstrating that the *ACE1* sensitivity is not a general property of chelators.

These data suggest that a ZPT-mediated increase in cellular copper leads to growth inhibition. This hypothesis was further supported by the finding that the potency of ZPT was increased by raising the copper concentration in the culture medium (Fig. 3b), resulting in a further increase in cellular copper content (see Table S5 in the supplemental material). In contrast, if copper is sequestered from the culture medium by the membrane-impermeable copper-specific chelator bathocuproine disulfonate (23), then the effect of ZPT becomes more attenuated (Fig. 3b) and there is no increase in cellular copper (see Fig. S1D in the supplemental material).

ZPT differed from the other chelators tested, as it was the most active of the chelators against an *ACE1* deletion strain and in raising intracellular copper levels. Further, ZPT was more potent in the presence of copper salts. For other chelators (octopirox, BPS, 1,10-phenanthroline, and EDTA), antiyeast activity was attenuated by the presence of copper salts (see Table S6 in the supplemental material), highlighting the unusual relationship between ZPT and copper.

ZPT affects Fe-S proteins. Genes that encode mitochondrial proteins were overrepresented among the ZPT-sensitive strains (51 of the 180 strains with growth reduced 2-fold by all three doses of ZPT in the deletion library screen) but not the zinc chloride-sensitive strains (32 of the 328 strains with growth reduced 2-fold by both doses of zinc chloride). With the deletion collection, increased ZPT sensitivity was observed for

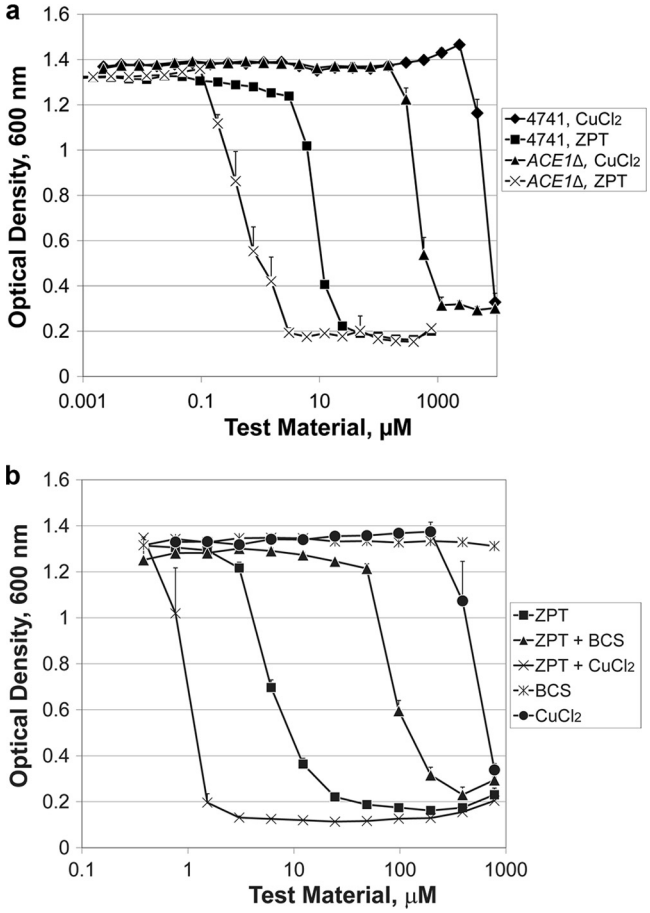

FIG. 3. ZPT activity is modulated by environmental copper and the copper resistance of the target yeast. (a) Sensitivity of wild-type and *ACE1* deletion mutant strains of *S. cerevisiae* to ZPT and copper chloride. The growth medium was YPD. Error bars represent one standard deviation; $n = 4$. (b) ZPT potency against *S. cerevisiae* BY4741 was influenced by the copper concentration. ZPT + BCS: BCS was held at 4.4 mM while the ZPT dose was adjusted as shown on the *x* axis. ZPT + $CuCl_2$: the $CuCl_2$ was held constant at 150 μM while the ZPT dose was adjusted as shown on the *x* axis. The growth medium was YPD. Error bars represent one standard deviation; $n = 2$.

strains with deletions in genes involved in Fe-S cluster synthesis. Of the seven genes known to function in transferring Fe-S clusters from the Isu1/2p scaffold to mitochondrial Fe-S proteins (21), five were ZPT sensitive, and the other two are essential genes and not represented in the deletion library. Four mutants with deletions in genes encoding mitochondrial Fe-S assembly (*IBA57*, *SSQ1*, *ISA1*, and *GRX5*) were among the 16 most ZPT-sensitive deletion mutants, while the fifth mutant with a deletion of a gene required for mitochondrial Fe-S protein assembly (*ISA2*) was the 47th most ZPT-sensitive deletion mutant. We extended these observations with tests of the ZPT sensitivity of a strain containing a hypomorphic allele of the essential *NFS1* gene as well as hypomorphs of *GSH2*, *MTM1*, and *ISU1*, all of which are involved in Fe-S cluster synthesis (19). All strains were more ZPT sensitive than the wild-type strain (see Fig. S2C and S2D in the supplemental material), providing further support of the hypothesis that ZPT targets Fe-S cluster-containing proteins.

Defects in Fe-S cluster assembly cause cells to be starved for glutamate and lysine, due to maturation defects of the Fe-S proteins aconitase and homoaconitase (14). Given that ZPT causes an apparent defect in Fe-S protein maturation, we asked whether the presence of lysine and glutamate would affect the potency of ZPT. When cells were grown in minimal medium, they were 10-fold less sensitive to ZPT when L-glutamate and L-lysine were added to the medium (Fig. 4a). In contrast, the D stereoisomer of these amino acids had no effect on ZPT potency. The addition of L-lysine provided nearly as much protection from ZPT as did the L form of both amino acids, suggesting that L-lysine provides most of the protection from ZPT and that ZPT affects glutamate and (especially) lysine synthesis due to inhibition of aconitase and/or homoaconitase activity. At the higher ZPT doses that inhibit growth in the presence of L-lysine and L-glutamate, one or more different targets must be inhibited by ZPT.

Reduction of iron-sulfur protein activity by ZPT. We tested whether there were any losses of Fe-S enzyme activity induced by ZPT treatment. When cultures were grown overnight in the presence of ZPT, there was less aconitase activity in cell lysates (Fig. 4b). For example, at 3 μM ZPT, a dose showing 13% ± 4% growth inhibition, aconitase specific activity was reduced to 7% ± 4% of level seen with the untreated sample. Decreased aconitase activity was also detected when cells were grown for times as short as 6 h (Fig. 4c). Growth in the presence of ZPT could cause aconitase activity loss by inhibition of the enzyme and/or by prevention of aconitase production. We tested whether there was inactive aconitase present in extracts from ZPT-treated cells by adding ferrous ammonium sulfate and dithiothreitol, a treatment known to restore activity to iron-depleted aconitase (3). Aconitase activity was recovered ($P < 0.01$ for a 3 μM ZPT dose), although it did not reach the level seen with untreated cells (Fig. 4b). This demonstrated the presence of inactivated aconitase and that the activity could be restored by the addition of iron and a reducing agent.

ZPT also induced decreases in the specific activity of other Fe-S-containing enzymes such as the cytosolic enzymes isopropylmalate isomerase (Leu1) and glutamate synthase (Fig. 4c). In contrast, there was little loss of specific activity for the mitochondrial enzyme malate dehydrogenase or the cytosolic zinc-containing enzyme alcohol dehydrogenase, each lacking Fe-S clusters (Fig. 4d). These data indicated that ZPT has a specific effect on the activity of Fe-S cluster-containing enzymes.

Relevance to *M. globosa*. To understand better how scalp fungi are affected by ZPT in antidandruff shampoos, we tested whether the ZPT-induced metal imbalance occurs in *M. globosa* as it does with the model yeast. Difficulties in culturing *M. globosa* in minimal medium have prevented us from testing whether glutamate and lysine auxotrophy is a target for growth inhibition such as was revealed in the *S. cerevisiae* experiments. There were similarities between the microarray studies of *M. globosa* and those of *S. cerevisiae*. With ZPT-treated *M. globosa*, the *CTR1* homolog was the fourth most downregulated gene. Furthermore, several iron starvation genes and a copper exporter homolog gene were upregulated (see Table S7 in the supplemental material).

Atomic emission data determined with *M. globosa* (Fig. 5a) showed that ZPT increased copper levels ($P < 0.02$) and de-

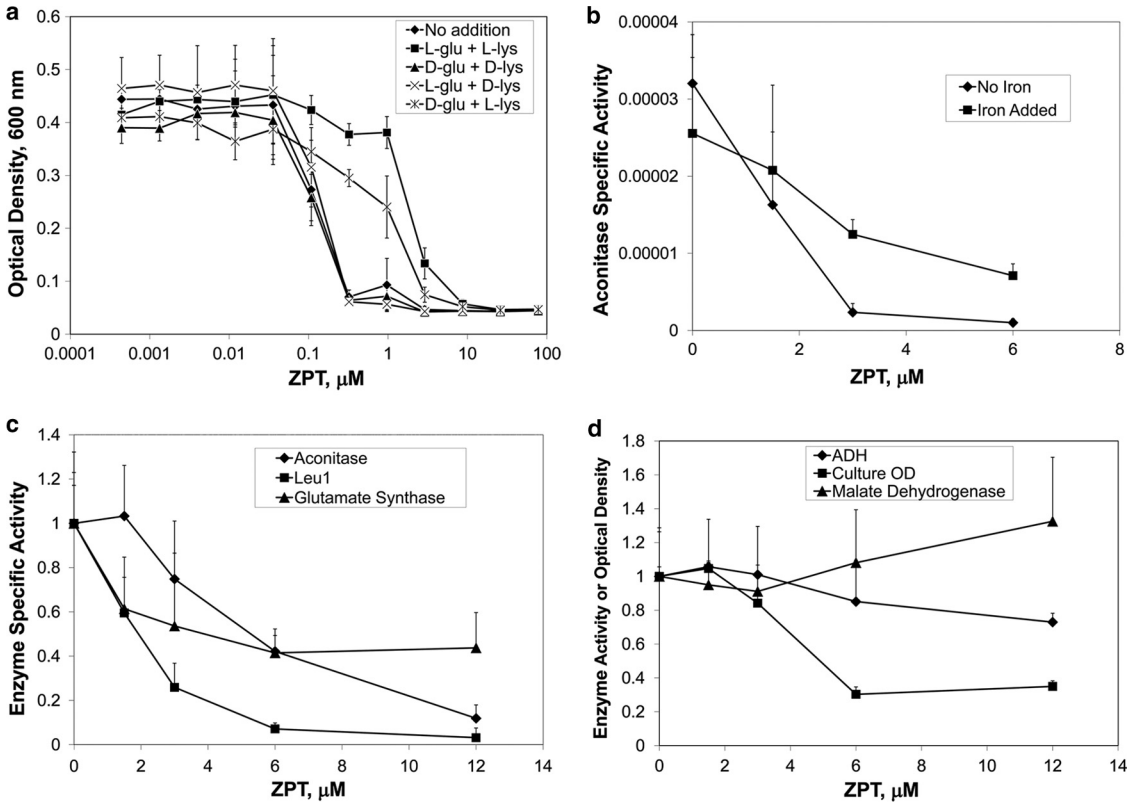

FIG. 4. ZPT targets Fe-S proteins. (a) ZPT was less potent in the presence of L-glutamate and L-lysine. BY4741 was cultured in YNB media (supplemented with histidine, leucine, methionine, and uracil to complement the auxotrophic markers) in the presence or absence of lysine and glutamate (40 μg/ml) and the indicated ZPT dose. Error bars represent one standard deviation; $n = 12$. (b) Aconitase inhibition by growth in the presence of ZPT. *S. cerevisiae* BY4741 was treated overnight with ZPT in YPD medium. The cells were lysed, and aconitase specific activity was measured. Error bars represent one standard deviation; $n = 3$. (c and d) ZPT reduces the specific activity of three Fe-S proteins (c) but not that of two proteins lacking Fe-S clusters (d). ADH, malate dehydrogenase. Error bars represent one standard deviation; $n = 3$.

creased iron levels ($P < 0.05$) and zinc levels ($P < 0.025$). Two other metal chelators, BPS and octopirox, when tested using *M. globosa*, each lowered cellular copper, iron, and zinc levels (see Table S8 in the supplemental material). The addition of copper improved the potency of ZPT against *M. globosa* (Fig. 5b). Based on the gene expression patterns and metal ion content and the influence of copper on ZPT potency, we conclude that *M. globosa* and *S. cerevisiae* show similar responses to ZPT.

DISCUSSION

Despite decades of commercial use of ZPT and several reports of its mechanism of action, this is the first report demonstrating that copper influx is part of ZPT's mechanism of action. ZPT inhibited fungal growth through an increase in cellular copper levels that was demonstrated in several ways. First, the downregulation of the *CTR1* copper importer gene, upregulation of the *CUP1* metallothionein gene, and atomic absorption spectroscopy measurements together indicated that the ZPT-treated cells contained increased copper levels. Second, deletion of *ACE1*, which protects cells from copper toxicity, rendered cells sensitive to ZPT, showing that the increased copper is biologically active. Third, ZPT was more potent when copper was added to the medium, and the cellular copper levels were higher than those seen with ZPT treatment alone, indicating that copper availability correlates with ZPT growth inhibition efficacy. Furthermore, when copper was sequestered by the copper-specific chelator bathocuproine disulfonate, ZPT became less potent and did not raise cellular copper levels.

According to data from the Irving-Williams series, copper is the metal with highest affinity to pyrithione and would be expected to replace zinc. Although copper influx has a role in ZPT-mediated growth inhibition, increased copper levels alone cannot account for growth inhibition. Yeast can grow in copper sulfate concentrations where the cell-associated copper amounts are 7-fold higher than that observed with growth-inhibitory doses of ZPT. In our model, ZPT dissociates and forms CuPT from available extracellular copper (Fig. 6). Pyrithione acts as an ionophore, interacting nonspecifically with the plasma membrane and shuttling copper into the cell. We speculate that pyrithione mediates copper transport across intracellular membranes, enabling copper to disperse throughout the cell, gaining access to intracellular organelles such as mitochondria. There is a precedent for pyrithione-mediated ionophore activity across intracellular membranes, as it was previously reported that pyrithione affected zinc transport across vacuole vesicles *in vitro* (25).

Our data suggest that the effect of increased copper is to

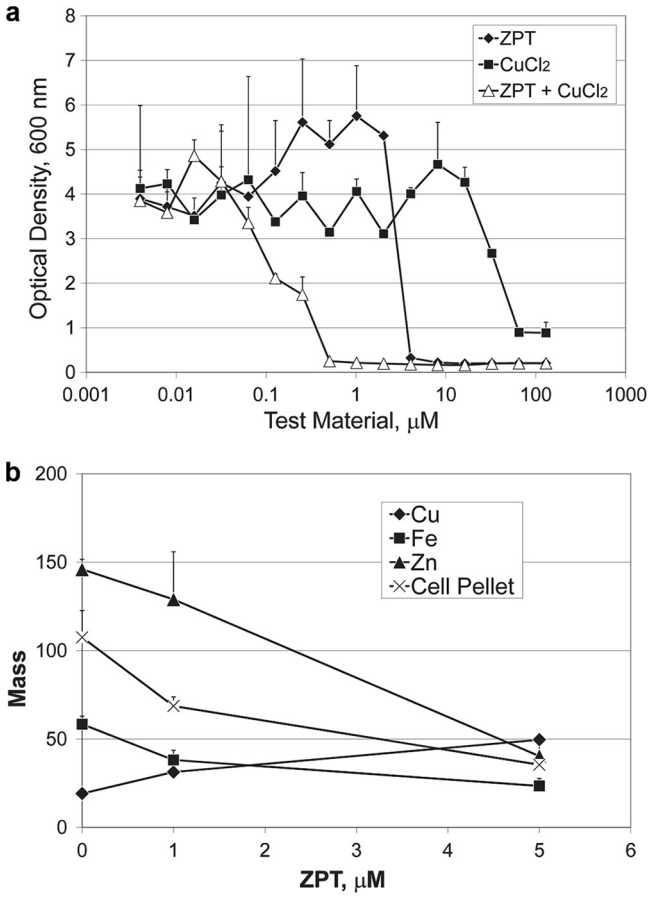

FIG. 5. ZPT targets *M. globosa* in a manner similar to its targeting of *S. cerevisiae*. (a) ZPT potency against *M. globosa* was influenced by medium copper concentration. The growth medium was mDixon. ZPT + $CuCl_2$: the *x* axis refers to the ZPT concentration, with $CuCl_2$ held constant at 1.2 mM. Error bars represent one standard deviation, $n = 2$. (b) Atomic emission spectroscopy of metal content after ZPT treatment of *M. globosa*. Cells (at an OD of 0.1) were dosed with the indicated amount of ZPT in minimal medium and incubated for 4 days at 31°C. Zinc and iron are reported in parts per million and copper in parts per 10 million. Cell pellet masses are reported as milligrams. Error bars represent one standard deviation, $n = 2$.

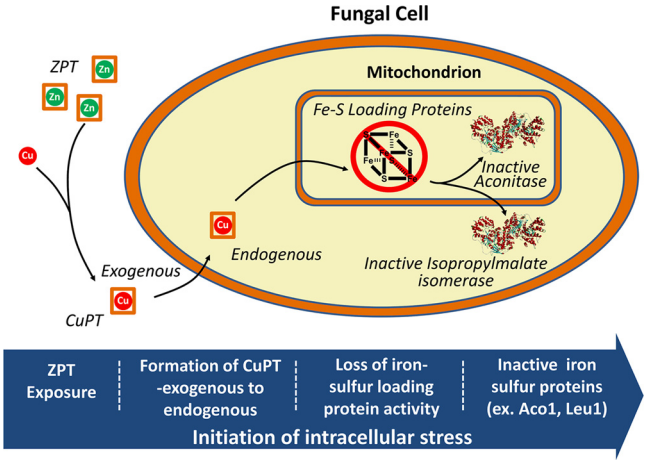

FIG. 6. A model for the inactivation of the representative Fe-S proteins aconitase (Aco1) and isopropylmalate isomerase (Leu1). Some of the pyrithione exchanges zinc for copper and transports copper across the plasma membrane and intracellular membranes. The Fe-S protein assembly is damaged, leading to loss of Aco1 and Leu1 activity.

decrease the activity of Fe-S cluster-containing enzymes. Fe-S protein maturation was the strongest theme among ZPT-sensitive mutants in the deletion library, and the enzymatic activities of several Fe-S proteins (aconitase, glutamate synthase, Leu1) were inhibited by growth in the presence of ZPT. In contrast, the activity of a wide variety of enzymes, including copper-containing enzymes (Sod1, Fet3), a manganese-containing enzyme (Sod2), a zinc-containing enzyme (alcohol dehydrogenase), and a metal-independent enzyme (malate dehydrogenase), was unaffected by ZPT treatment. The finding that ZPT affects Fe-S clusters is consistent with recent reports that the molecular mechanism of copper toxicity in *Escherichia coli* (26) and *Bacillus subtilis* (7) is loss of Fe-S cluster enzyme activity. Many of the enzymes involved in the synthesis of Fe-S cluster-containing enzymes are themselves Fe-S cluster-containing proteins. Pyrithione may enable some copper to enter the mitochondria. We propose that, once it is inside the mitochondria, copper inactivates Fe-S protein maturation, the targets identified in our deletion library analysis. Indeed, the distribution of copper within subcellular organelles may explain the limited increase of *CUP1* transcription, suggesting that cytoplasmic copper levels are not much elevated. In future research, it would be useful to measure the copper content of intracellular organelles.

Defects in Fe-S assembly can lead to increased *FET3* expression favoring iron uptake (19) and may explain increased expression of the iron regulon, as seen here and previously reported by Yasokawa et al. (43). We observed a ZPT-mediated increase in iron uptake but not an increase in accumulated iron levels. This inconsistency may be due to export of Fe-S clusters that have been damaged by ZPT treatment. Decreased cellular iron is seen in mammalian cells treated with nitric oxide and appears to result from the export of Fe-S clusters by multidrug-resistant transporters (40). Induction of multidrug transport genes in *S. cerevisiae* is also associated with decreased cellular iron levels even in the face of increased iron transport activity (38).

Yasokawa et al. (43) reported that a high (2 mM) dose of iron reduces the potency of ZPT, with the interpretation that iron starvation is at least part of the mechanism of action of ZPT. An alternative explanation is that large amounts of iron compete effectively with copper for pyrithione, resulting in less CuPT to inhibit yeast growth.

The described activity of ZPT against *S. cerevisiae* is likely relevant to the antifungal effects against *M. globosa*, as we observed increases in cellular copper levels and in the transcriptional response expected with high copper concentrations and an increase in ZPT potency in the presence of elevated copper levels. While it seems likely that Fe-S clusters are the targets of ZPT activity against *M. globosa*, we have not overcome the challenges of experimentation with this organism to resolve this hypothesis.

The concentration of free copper within bacteria or single-cell eukaryotes is vanishingly small (32). As shown here, depletion of extracellular copper reduces the growth-inhibitory

effect of ZPT. These results lead to the issue of determining the source of copper for ZPT activity during shampoo use. The results of a recent study demonstrating that mycobacterial virulence involves copper resistance (41) indicate that increased copper concentrations in phagosomes might be a source of copper for macrophage-induced bactericidal and perhaps fungicidal activity. We wonder whether increasing available copper levels represent a general property of the antimicrobial response of the immune system and whether the antifungal activity of ZPT for the scalp could be attributed to its action in concert with copper supplied by the immune system. Alternatively, copper may be released during the skin renewal process, in which epithelial cells lose their integrity as they approach the skin surface.

ACKNOWLEDGMENTS

We thank Kevin Mills, Erica Kincaid, Angie Boyer, Jim Thompson, Chris Kelling, and Bob LeBoeuf for their support and Dongmei Ren and members of the Kaplan laboratory for experimental assistance. We thank the two anonymous reviewers, whose comments prompted improvement of the manuscript.

Some of the work performed in the Kaplan laboratory was supported by NIH grant DK052380.

REFERENCES

1. **Andersson, D. A., C. Gentry, S. Moss, and S. Bevan.** 2009. Clioquinol and pyrithione activate TRPA1 by increasing intracellular Zn^{2+}. Proc. Natl. Acad. Sci. U. S. A. **106:**8374–8379.
2. **Askwith, C., et al.** 1994. The FET3 gene of S. cerevisiae encodes a multicopper oxidase required for ferrous iron uptake. Cell **76:**403–410.
3. **Beinert, H., and M. C. Kennedy.** 1989. Engineering of protein bound iron-sulfur clusters. A tool for the study of protein and cluster chemistry and mechanism of iron-sulfur enzymes. Eur. J. Biochem. **186:**5–15.
4. **Blandino, A., I. Caro, and D. Cantero.** 1997. Comparative study of alcohol dehydrogenase activity in flour yeast extracts. Biotechnol. Lett. **19:**651–654.
5. **Chandler, C. J., and I. H. Segel.** 1978. Mechanism of the antimicrobial action of pyrithione: effects on membrane transport, ATP levels, and protein synthesis. Antimicrob. Agents Chemother. **14:**60–68.
6. **Chen, T. A., and P. B. Hill.** 2005. The biology of Malassezia organisms and their ability to induce immune responses and skin disease. Vet. Dermatol. **16:**4–26.
7. **Chillappagari, S., et al.** 2010. Copper stress affects iron homeostasis by destabilizing iron-sulfur cluster formation in Bacillus subtilis. J. Bacteriol. **192:**2512–2524.
8. **Davis-Kaplan, S. R., C. C. Askwith, A. C. Bengtzen, D. Radisky, and J. Kaplan.** 1998. Chloride is an allosteric effector of copper assembly for the yeast multicopper oxidase Fet3p: an unexpected role for intracellular chloride channels. Proc. Natl. Acad. Sci. U. S. A. **95:**13641–13645.
9. **DeAngelis, Y. M., et al.** 2007. Isolation and expression of a Malassezia globosa lipase gene, LIP1. J. Investig. Dermatol. **127:**2138–2146.
10. **De Freitas, J. M., A. Liba, R. Meneghini, J. S. Valentine, and E. B. Gralla.** 2000. Yeast lacking Cu-Zn superoxide dismutase show altered iron homeostasis. Role of oxidative stress in iron metabolism. J. Biol. Chem. **275:**11645–11649.
11. **Ermolayeva, E., and D. Sanders.** 1995. Mechanism of pyrithione-induced membrane depolarization in Neurospora crassa. Appl. Environ. Microbiol. **61:**3385–3390.
12. **Felice, M. R., et al.** 2005. Post-transcriptional regulation of the yeast high affinity iron transport system. J. Biol. Chem. **280:**22181–22190.
13. **Gaxiola, R. A., D. S. Yuan, R. D. Klausner, and G. R. Fink.** 1998. The yeast CLC chloride channel functions in cation homeostasis. Proc. Natl. Acad. Sci. U. S. A. **95:**4046–4050.
14. **Gelling, C., I. W. Dawes, N. Richhardt, R. Lill, and U. Muhlenhoff.** 2008. Mitochondrial Iba57p is required for Fe/S cluster formation on aconitase and activation of radical SAM enzymes. Mol. Cell. Biol. **28:**1851–1861.
15. **Gemmer, C. M., Y. M. DeAngelis, B. Theelen, T. Boekhout, and T. L. Dawson, Jr.** 2002. Fast, noninvasive method for molecular detection and differentiation of Malassezia yeast species on human skin and application of the method to dandruff microbiology. J. Clin. Microbiol. **40:**3350–3357.
16. **Gross, C., M. Kelleher, V. R. Iyer, P. O. Brown, and D. R. Winge.** 2000. Identification of the copper regulon in Saccharomyces cerevisiae by DNA microarrays. J. Biol. Chem. **275:**32310–32316.
17. **Hollander, M., and D. A. Wolfe.** 1999. Nonparametric statistical methods, 2nd ed. John Wiley & Sons, New York, NY.
18. **Krenn, B. M., et al.** 2009. Antiviral activity of the zinc ionophores pyrithione and hinokitiol against picornavirus infections. J. Virol. **83:**58–64.
19. **Kumánovics, A., et al.** 2008. Identification of FRA1 and FRA2 as genes involved in regulating the yeast iron regulon in response to decreased mitochondrial iron-sulfur cluster synthesis. J. Biol. Chem. **283:**10276–10286.
20. **Li, L., and J. Kaplan.** 2004. A mitochondrial-vacuolar signaling pathway in yeast that affects iron and copper metabolism. J. Biol. Chem. **279:**33653–33661.
21. **Lill, R.** 2009. Function and biogenesis of iron-sulphur proteins. Nature **460:**831–838.
22. **Lin, H., et al.** 2008. A single amino acid change in the yeast vacuolar metal transporters ZRC1 and COT1 alters their substrate specificity. J. Biol. Chem. **283:**33865–33873.
23. **Lynch, S. M., and B. Frei.** 1995. Reduction of copper, but not iron, by human low density lipoprotein (LDL). Implications for metal ion-dependent oxidative modification of LDL. J. Biol. Chem. **270:**5158–5163.
24. **MacDiarmid, C. W., L. A. Gaither, and D. Eide.** 2000. Zinc transporters that regulate vacuolar zinc storage in Saccharomyces cerevisiae. EMBO J. **19:**2845–2855.
25. **MacDiarmid, C. W., M. A. Milanick, and D. J. Eide.** 2002. Biochemical properties of vacuolar zinc transport systems of Saccharomyces cerevisiae. J. Biol. Chem. **277:**39187–39194.
26. **Macomber, L., and J. A. Imlay.** 2009. The iron-sulfur clusters of dehydratases are primary intracellular targets of copper toxicity. Proc. Natl. Acad. Sci. U. S. A. **106:**8344–8349.
27. **Magda, D., et al.** 2008. Synthesis and anticancer properties of water-soluble zinc ionophores. Cancer Res. **68:**5318–5325.
28. **Pagani, M. A., A. Casamayor, R. Serrano, S. Atrian, and J. Arino.** 2007. Disruption of iron homeostasis in Saccharomyces cerevisiae by high zinc levels: a genome-wide study. Mol. Microbiol. **65:**521–537.
29. **Peña, M. M. O., K. A. Koch, and D. J. Thiele.** 1998. Dynamic regulation of copper uptake and detoxification genes in Saccharomyces cerevisiae. Mol. Cell. Biol. **18:**2514–2523.
30. **Pierik, A. J., D. J. Netz, and R. Lill.** 2009. Analysis of iron-sulfur protein maturation in eukaryotes. Nat. Protoc. **4:**753–766.
31. **Pierrel, F., P. A. Cobine, and D. R. Winge.** 2007. Metal Ion availability in mitochondria. Biometals **20:**675–682.
32. **Rae, T. D., P. J. Schmidt, R. A. Pufahl, V. C. Culotta, and T. V. O'Halloran.** 1999. Undetectable intracellular free copper: the requirement of a copper chaperone for superoxide dismutase. Science **284:**805–808.
33. **Ramsay, L. M., and G. M. Gadd.** 1997. Mutants of Saccharomyces cerevisiae defective in vacuolar function confirm a role for the vacuole in toxic metal ion detoxification. FEMS Microbiol. Lett. **152:**293–298.
34. **Reisch, A. S., and O. Elpeleg.** 2007. Biochemical assays for mitochondrial activity: assays of TCA cycle enzymes and PDHc. Methods Cell Biol. **80:**199–222.
35. **Roon, R. J., H. L. Even, and F. Larimore.** 1974. Glutamate synthase: properties of the reduced nicotinamide adenine dinucleotide-dependent enzyme from Saccharomyces cerevisiae. J. Bacteriol. **118:**89–95.
36. **Schwartz, J. R., C. W. Cardin, and T. L. Dawson.** 2004. Dandruff and seborrheic dermatitis, p. 259–272. *In* R. Baran and H. I. Maibach (ed.), Textbook of cosmetic dermatology. Martin Dunitz, Ltd., London, United Kingdom.
37. **Thomas, K. V.** 1999. Determination of the antifouling agent zinc pyrithione in water samples by copper chelate formation and high-performance liquid chromatography-atmospheric pressure chemical ionisation mass spectrometry. J. Chromatogr. A **833:**105–109.
38. **Tuttle, M. S., D. Radisky, L. Li, and J. Kaplan.** 2003. A dominant allele of PDR1 alters transition metal resistance in yeast. J. Biol. Chem. **278:**1273–1280.
39. **van Bakel, H., E. Strengman, C. Wijmenga, and F. C. Holstege.** 2005. Gene expression profiling and phenotype analyses of S. cerevisiae in response to changing copper reveals six genes with new roles in copper and iron metabolism. Physiol. Genomics **22:**356–367.
40. **Watts, R. N., C. Hawkins, P. Ponka, and D. R. Richardson.** 2006. Nitrogen monoxide (NO)-mediated iron release from cells is linked to NO-induced glutathione efflux via multidrug resistance-associated protein 1. Proc. Natl. Acad. Sci. U. S. A. **103:**7670–7675.
41. **Wolschendorf, F., et al.** 2011. Copper resistance is essential for virulence of Mycobacterium tuberculosis. Proc. Natl. Acad. Sci. U. S. A. **108:**1621–1626.
42. **Xu, J., et al.** 2007. Dandruff-associated Malassezia genomes reveal convergent and divergent virulence traits shared with plant and human fungal pathogens. Proc. Natl. Acad. Sci. U. S. A. **104:**18730–18735.
43. **Yasokawa, D., et al.** 2010. DNA microarray analysis suggests that zinc pyrithione causes iron starvation to the yeast Saccharomyces cerevisiae. J. Biosci. Bioeng. **109:**479–486.
44. **Yasokawa, D., et al.** 2008. Mechanisms of copper toxicity in Saccharomyces cerevisiae determined by microarray analysis. Environ. Toxicol. **23:**599–606.
45. **Zhao, H., et al.** 1998. Regulation of zinc homeostasis in yeast by binding of the ZAP1 transcriptional activator to zinc-responsive promoter elements. J. Biol. Chem. **273:**28713–28720.